EASR

Synthesis of microcrystalline cellulose from banana pseudo-stem for adsorption of organics from aqueous solution

Trung Thanh Nguyen*[1, 2)], Bao Tran Nguyen Thi[1, 2)], Phuoc Toan Phan[1, 2, 3)], Tri Thich Le[1, 2)], Quynh Anh Nguyen Thi[1, 2)], Long Giang Bach[4)], Thai Anh Nguyen[5)] and Nhat Huy Nguyen*[2,3)]

[1)]Nanomaterial Laboratory, An Giang University, 18 Ung Van Khiem St, Dong Xuyen Dist, Long Xuyen City, An Giang Province, Vietnam
[2)]Vietnam National University Ho Chi Minh City, Linh Trung Ward, Thu Duc District, Ho Chi Minh City, Vietnam
[3)]Faculty of Natural Resources and Environment, Ho Chi Minh City University of Technology (HCMUT), 268 Ly Thuong Kiet St, Dist. 10, Ho Chi Minh City, Vietnam
[4)]NTT Institute of High Technology, Nguyen Tat Thanh University, 298-300A Nguyen Tat Thanh, Ho Chi Minh City, Vietnam
[5)]Faculty of Chemical and Food Technology, Ho Chi Minh City University of Technology and Education, 01 Vo Van Ngan St, Thu Duc Dist, Ho Chi Minh City, Vietnam

Abstract

In this study, we proposed and tested a green method for producing microcrystalline cellulose (MCC) with high quality from waste banana pseudo-stem (BPS) after fruit harvesting. The MCC was synthesized by treating BPS with sulfuric acid, sodium hydroxide, and H_2O_2 solution. The produced MCC material was then characterized by scanning electron microscopy, Fourier transform infrared spectroscopy, X-ray diffraction, and thermogravimetric analysis to explore its properties. The removal of methylene blue (MB) in aqueous solution was conducted by batch adsorption method to evaluate the applicability of MCC for wastewater treatment. The results showed that the adsorption using MCC reached equilibrium after 15 min. The highest MB adsorption capacity of MCC reached 16.6 mg/g at pH 6. The adsorption kinetics data were best described by the pseudo second order rate equation. Equilibrium isotherm data of adsorption were well fitted to the linear Langmuir isotherm model. Affecting factors such as adsorbent dosage, initial concentration of MB, and temperature were also investigated. These results suggest a great potential use of MCC for advanced wastewater treatment.

Keywords: Microcrystalline cellulose, Adsorption, Banana pseudo-stem, Methylene blue, Wastewater treatment

1. Introduction

Banana is one of the most popular food crops, particularly in tropical countries [1, 2]. After fruit harvesting, banana wastes including pseudo-stems, leaves, piths, and even fruit peels are left in the farm or disposed into the environment, which could cause water pollution and release greenhouse gas [3]. Due to its abundance and high carbon content, the banana wastes have been studied intensively as an adsorbent for water treatment such as removal of metal ions, dyes, pesticides, inorganic cations, and other organic compounds in water and wastewater [2, 4, 5]. Recently, microcrystalline cellulose (MCC) has emerged as a very promising natural material with many applications in food, binder, medical, and cosmetic industries [6-8]. There are some methods for the extraction of cellulose such as physical, chemical, biological, or combined methods. These methods are usually used as a pretreatment step for the hydrolysis step in the MCC synthesis, such as acid hydrolysis, alkali hydrolysis, steam explosion, extrusion, and radiation-enzymatic methods [8]. The addition of hydrogen peroxide in the alkali hydrolysis method was also proposed to reduce the viscosity and thus effective for MCC production [9]. There have been some studies on the production of MCC from banana wastes [10-19]. Activated carbon was prepared from used banana pseudo-stem by phosphoric chemical activation, which was used to remove methylene blue (MB) dye from synthetic dye solution [10]. The adsorption of hexavalent chromium into activated carbon derived from acrylonitrile-divinylbenzene was maximum at low pH and high temperature. Adsorption mechanisms were studied by X-ray photoelectron spectroscopy [11]. Microcrystalline cellulose (MCC) was prepared by hydrolyzing banana fiber wastes [12, 13]. In Egypt, MCC was from renewable biomass resources, rice straw, and banana plant waste. MCC was then obtained by enzymatic treatment resulting in cellulose [14, 15]. Banana pseudo-stem was supplied by courtesy of J.K.U.A.T farm. Preparation of the MCC was carried out using the alkali hydrolysis process followed by further treatment using peracetic acid [16]. Cellulosic banana fibers are potential engineering materials having considerable scope to be used as an environmentally friendly reinforcing element for manufacturing polymer-based green materials [17]. Cellulose nanofibers were isolated from banana peel using a combination of chemical treatments such as alkaline treatment, bleaching, and acid hydrolysis. All treatments effectively isolated banana fibers in the nanometer scale [18, 19]. The lignocellulosic contents in banana pseudo-stem were reported to be around 64 % [20] and 60-85% [21], which was relatively higher than other wastes and could be very potential for MCC production in practical. There are many studies on the application of MCC for the removal of

metals and dyes, the use of MCC for dye adsorption is preferred due to their similar properties of organics and the easy management of the adsorbed material [22]. Additionally, for MCC activation, the chemicals with strong oxidation properties (e.g., $HOCl_4$) are usually used in the MCC synthesis procedure; therefore, the green generation MCC without using toxic chemicals is also the motivation for the next studies. In this study, we use the waste banana pseudo-stem (after harvesting fruits) for producing microcrystalline cellulose since the MCC is more effective and easy for separation after adsorption. The use of H_2O_2 as an activated agent is considered as a green process that does not require toxic chemicals and reduce the release of polluted wastewater after the MCC generation process.

In this work, the banana strain used in this study is the Siamese banana, which was collected from a farm located in the south of Vietnam. Siamese bananas are a very popular banana strain in Vietnam with a huge production yield. Compared with other types of post-harvest waste from banana, the banana pseudo-stem is the organ with the largest volume of waste from the banana tree, so it was selected as the main study subject. Microcrystalline cellulose (MCC) was prepared from waste banana pseudo-stem by extraction method.

Material characterization was done to explore the microstructure and properties of the MCC product. The application of produced MCC was evaluated by its ability as an adsorbent for MB in water. The effect of environmental factors on the MB adsorption capacity of MCC material was investigated and the kinetics of adsorption was also studied.

2. Experimental

2.1. Material preparation and characterization

Analytical grade chemicals including H_2SO_4, NaOH, H_2O_2 (35% w/w), and MB (Germany) were purchased in Ho Chi Minh City (Vietnam). Deionized (DI) water used in the study was taken from a deionization system in the laboratory. MCC extraction process from Pisang Awak BPS, which was collected from the banana-growing area in An Giang Province, Vietnam, was combined with chemical, physical, and thermal treatments to remove undesired lignin components as follows. Raw BPS was chopped up into small pieces with length in a range of 2 - 3 cm (Figure 1a). These small pieces were rinsed several times with tap water and were dried in a dry oven. The BPS pieces were then mixed with 2 N H_2SO_4 solution (in a ratio of 1:10 in weight) and followed by refluxing for 1 h to extract cellulose. The extracted fibers were subsequently washed with DI water several times until the pH reached 7 (Figure 1b). After treatment with acid, the material was refluxed with 10% (w/w) NaOH solution under the same condition as treatment with acid and was experienced drying for 3 to 4 h at 50 ºC in a dry oven afterward (Figure 1c). The dried material was then treated with a 35% H_2O_2 solution overnight to remove the remained lignin and hemicellulose. The material was finally washed with DI water, dried at 50 ºC, and crushed into powder (Figure 1d).

Various techniques were employed for the characterization of MCC material such as scanning electron microscopy (SEM), Fourier transform infrared spectroscopy (FTIR), X-ray diffraction (XRD), thermogravimetric analysis (TGA), and Brunauer-Emmett-Teller (BET) method. FTIR spectra were obtained using a Bruker-FTIR with spectrum scanned from 500 to 4,000 cm^{-1}. TGA was conducted by using a TGA Q500 machine in ambient conditions at a rate of 10 ºC/min and a temperature range of 30-800 ºC. The specific surface area was determined using a BET-202A machine (Porous Materials). The details of these techniques as well as sample preparation and equipment can be found in the literature [23].

X-ray diffraction (XRD) were recorded for sample powder using a D2 Phaser XRD 300 W diffractometer equipped with Cu Kα radiation (λ = 1.5406 A) at a step size of 0.01º and step time of 30 s. The percentage of crystallinity index (CrI) was calculated using following quation [24]: $CrI = \frac{I_{002} - I_{am}}{I_{002}}$

Where I_{002} represents the peak intensity corresponding to the crystalline domain (20º to 19º) and I_{am} represents the peak intensity corresponding to the amorphous domain (2º to 22.6º).

The point of zero charge (pH_{pzc}) of the material was determined followed a process published in the literature [25]. In brief, a series of 50 mL of 0.01 N KCl solution with initial pH (pH_o) from 2 to 12 were prepared by adding 0.1 M HCl or 0.1 M NaOH solution. These solutions were then added with 0.1 g MCC, shaken well, and let stable for 48 h. The suspension was then filtrated and measure the final pH values (pH_t). The point of zero charge was determined as the $\Delta pH = pH_0 - pH_t$ is closed to zero [26].

Figure 1 Pictures of (a) raw banana pseudo-stem, (b) after treating with H_2SO_4, (c) after treating with NaOH, and (d) final product after treating with H_2O_2

2.2. Adsorption test

In a typical process, each 50 mL of 10 ppm MB at pH 7 and room temperature (~ 30 °C) was transferred to every six 100-mL Erlenmeyer flasks containing 30 mg of MCC. The mixtures were then stirred and shaken by an orbital shaker for every separate 5, 10, 15, 20, 25, 30, and 60 min. After shaking, the extraction solution of each Erlenmeyer flask was immediately collected into cuvettes for MB concentration measurement by a spectrophotometer with a maximum absorbance peak of $\lambda_{max} = 664$ nm for each sample (Specord 210 plus, Analytik Jena). Other affecting factors were also investigated, including pH (3, 4, 5, 6, 7, 8, 9, and 10), amounts of MCC (10, 20, 30, 40, 50, and 60 mg), concentrations of MB (5, 10, 20, 30, and 40 mg/L), and temperatures (20, 25, 30, 35, 40, and 45 °C). All experiments were replicated three times and the adsorption capacity was calculated as follows:

$$Q = \frac{C_0 - C_e}{m} \times V \tag{1}$$

$$R\% = \frac{C_0 - C_t}{C_0} \times 100 \tag{2}$$

Where Q (mg/g) is the adsorption capacity and R% is removal efficiency. C_o, C_t, and C_e (mg/L) are the initial, at time t, and equilibrium MB concentrations in the aqueous solution, respectively. V (50 mL) is the volume of the experimental solution and m (g) is the adsorbent weight.

Some kinetic models were tested to check the interaction between MB and MCC adsorbent over time [27]. This study investigated 3 models including (1-3):

Pseudo-first-order: $\ln(Q - Q_t) = \ln Q - k_1 t$ \hfill (3)

Pseudo-second-order: $\frac{t}{Q_t} = \frac{1}{k_2 Q^2} + \frac{t}{Q}$ \hfill (4)

Intra-particle diffusion: $Q_t = k_{ip} t^{0.5}$ \hfill (5)

Where Q (mg/g) and Q_t (mg/g) are adsorption capacity of MCC at equilibrium and time t (min), and k_1 (min^{-1}), K_1 (min^{-1}), k_2 (g mg^{-1} min^{-1}) and k_p (mg g^{-1} min^{-1}) are the rate constant of pseudo first order model, modified pseudo first order model, pseudo second order model, and intraparticle diffusion model, respectively

The Langmuir isotherms assume monolayer adsorption without the interaction between the adsorbate [27], as following:

$$Q = \frac{K_L Q_{max} C_e}{1 + K_L C_e} \tag{6}$$

$$\frac{C_e}{Q} = \frac{1}{K_L Q_{max}} + \frac{C_e}{Q_{max}} \tag{7}$$

Where C_e (mg/L) is the equilibrium concentration and Q (mg/g) is the adsorption capacity. Q_{max} (mg/g) is the maximum adsorption capacity and K_L (L/mg) is the adsorption constant.

The Freundlich isotherms is expressed as following [28]:

$$Q = K_F C_e^{1/n} \tag{8}$$

$$\ln Q = \ln K_F + \frac{1}{n} \ln C_e \tag{9}$$

Where K_F and n are Freundlich constants.

The thermodynamic study was also done, based on the following equations [27]:

$$\Delta G = -RT \ln K \tag{10}$$

$$\Delta G = \Delta H - T\Delta S \tag{11}$$

$$K = \frac{Q}{C_e} \tag{12}$$

$$\ln K = \frac{\Delta S}{R} - \frac{\Delta H}{R} \times \frac{1}{T} \tag{13}$$

Where ΔG is free Gibb energy (kJ/mol) and T is the temperature (K). R is the gas constant (8.314 × 10-3 kJ/K.mol) and K is the constant [29]. C_e is the equilibrium concentration in the solution (mmol/mL) and Q is the adsorption capacity (mg/g).

For the generation of MCC material after MB adsorption, the MB-saturated MCC was soaked into the 0.1 M NaOH solution for 60 min. The reactivated MCC was then separated and washed with DI water, dried at 50 °C. It was noted that the ratio of MB-saturated MCC: NaOH solution was 1 gram: 50 mL.

3. Results and discussion

3.1. Material synthesis and characterization

The morphology of MCC material was studied with SEM, which are exhibited in Figure 2 at different levels of resolution. It was observed that the produced MCC was in the form of microfibrils and a high breakdown of cellulose chains. The MCC material has a white color and consists of fibers with a length of around 15 - 20 µm, which is consistent with previous reports [30, 31]. The BET surface area was measured to be 9.59 m^2/g, which was relatively high and potential for adsorption application. The surface chemical properties of MCC material (before and after adsorption) were determined by FTIR analysis [32]. As can be seen in Figure 3, FTIR results showed the cellulose form of carbohydrate of MCC material with FTIR peaks at wave numbers of 890, 1050, and 1420 cm^{-1} of CH rocking vibration, CO stretching, and CH$_2$ bending vibration, respectively. Besides, peaks at the wavenumber of 1620 cm^{-1} and 3420 - 3445 cm^{-1} were the stretching vibrations of absorbed water [33], while the peak at 2910 cm^{-1} was stretching vibration of CH [34-36]. The C-OH out-of-plane bending mode was observed at 667 cm^{-1} [37]. These indicate the successful preparation of MCC from BPS via this green method.
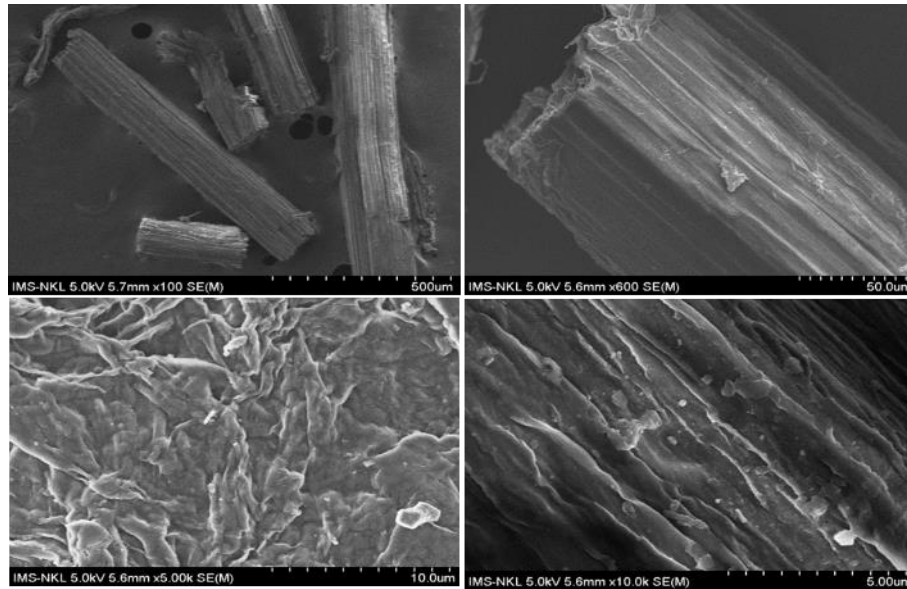
(a)
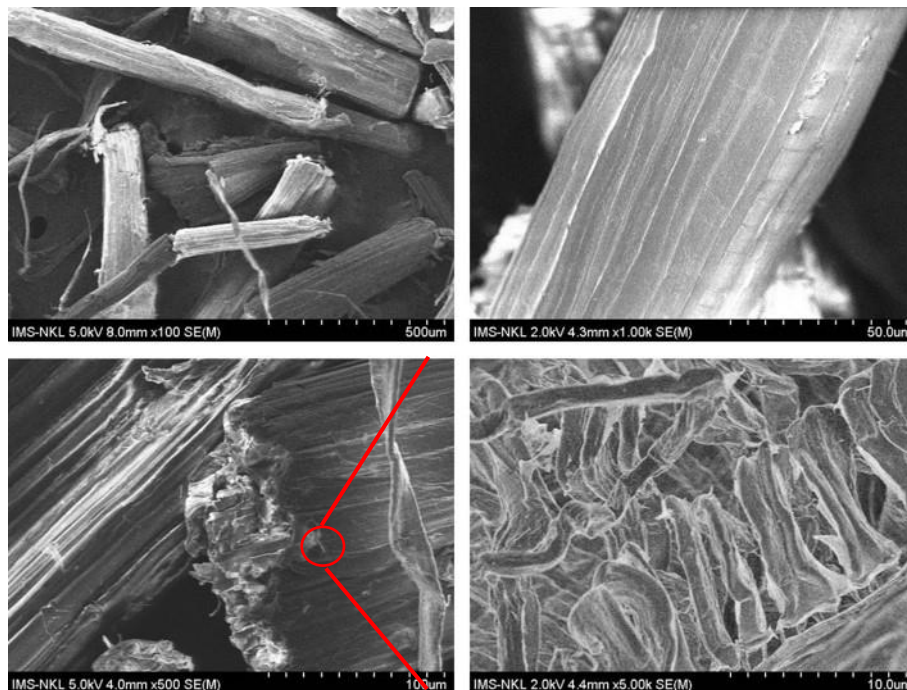
(b)

Figure 2 (a) SEM images of MCC before treatment with hydrogen peroxide at different resolutions; (b) SEM images of MCC after treatment hydrogen peroxide at different levels of resolution
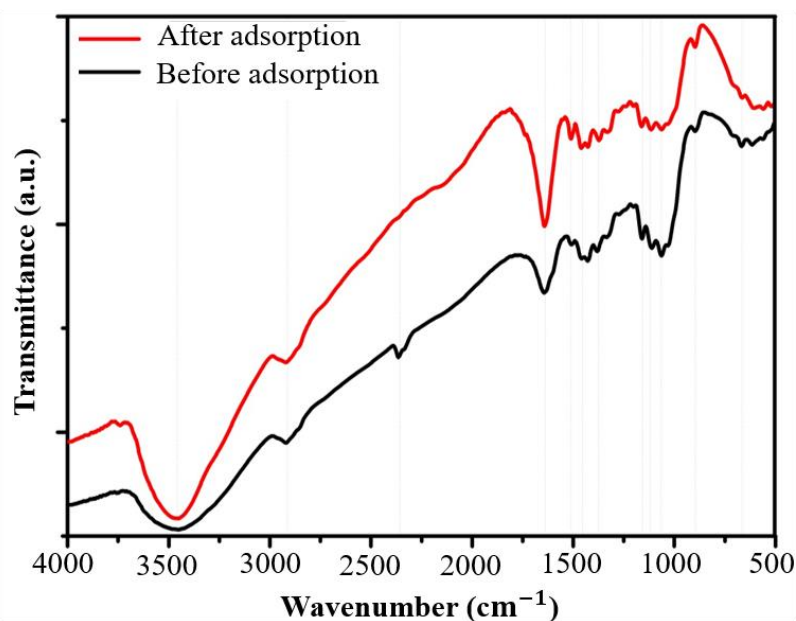
Figure 3 FTIR spectrum of MCC material before and after adsorption

Figure 4 depicts the thermal gravimetric results from thermal gravity analysis (TG) and differential thermogravimetric analysis (DTG) of MCC material. Results showed a thermal degradation of MCC prepared from BPS, which was similar to those reported in the literature for MCC produced from biomass [38, 39]. Three degradation stages are observed in this sample. The first stage of mass loss of around 10% from 50 – 200 °C is attributed to the water release. The second stage shows that MCC thermal decomposition occurred at a temperature range of 200-400 °C, which could be attributed to the depolymerization of cellulose [38] or the thermal decomposition of hemicelluloses/pectin. This was further confirmed by the presence of a more homogeneous crystal at a narrow peak of 312 °C in the DTG curve [40]. Previous literature has reported that the thermal decomposition of lignocellulosic material firstly happened with hemicelluloses, then with cellulose, and finally with lignin [39]. Moreover, this indicates that the MCC material only combines cellulose I with crystal structure [38]. The last mass loss in a temperature range of 420 - 600 °C is explained by the secondary reactions of carbon-containing residues [41] or the decomposition of lignin. The very low mass of 1.1% remained after 600 °C indicates the effective removal of fixed and inorganic components of BPS to produce relatively high quality of MCC.
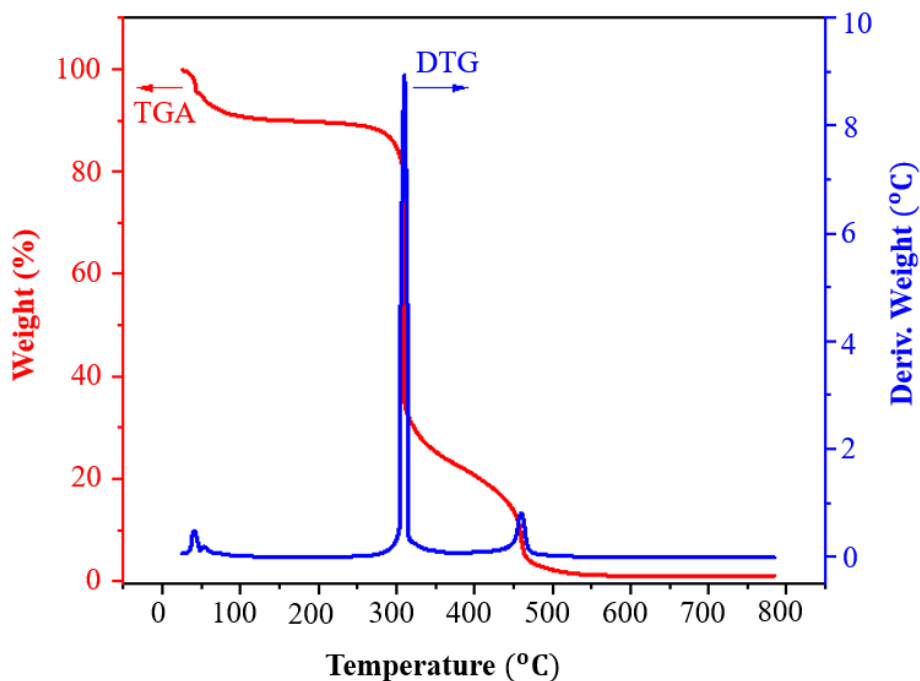

Figure 4 TGA – DTG curves of MCC

XRD technique was used to determine the crystallinity index of MCC material. In Figure 5, a sharp diffraction peak in 2θ of $19°$ - $23°$ indicates that MCC prepared from BPS has a crystalline structure, which is similar to MCC produced from palm biomass [35], rice husk [42], and cotton fiber [43]. The peak at 2θ of $22°$ was the characteristic peak of crystalline cellulose (2 0 0) which was classified into cellulose I (as also found by DTG) because of the absence of doublet in this peak [42]. Furthermore, three other peaks were also observed at 2θ of $14°$, $16°$, and $34°$ related to the crystallographic planes of (1 0 1), (1 1 0), and (0 0 4). The cellulose crystallinity index (CrI) calculated from XRD peak of the prepared MCC was 91.2%, which is relatively high in comparison with MCC from palm biomass (88%), rice husk (67%), wood (71%), and rice straw (68%) [10, 35, 42, 44, 45].
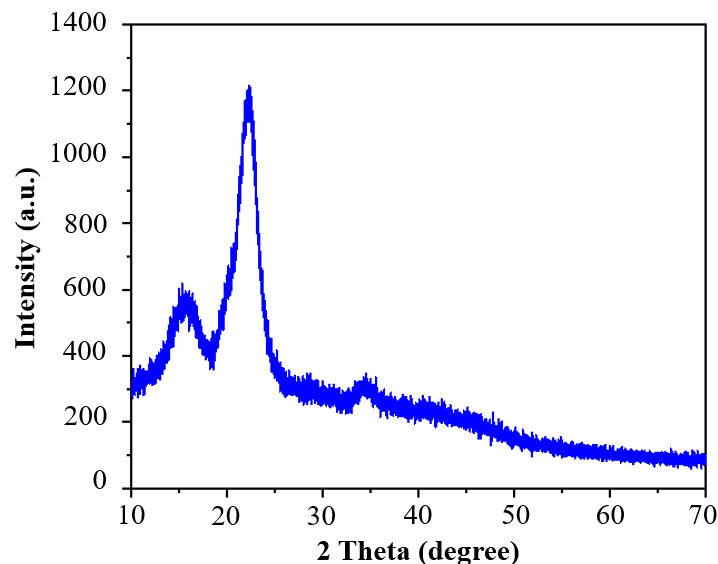

Figure 5 XRD pattern of MCC

3.2. Adsorption of MB

The effect of adsorption time on MB adsorption capacity of MCC material is displayed in Figure 6. It is clearly seen that the adsorption capacity of the material increased rapidly in the first 5 min and then increased slowly from 5 to 15 min. The adsorption process reached equilibrium after 15 min of the experiment and the highest MB adsorption capacity of the material was calculated at 13.5 mg/g. For comparison, the MB adsorption capacity of the MCC material without treatment with H_2O_2 was 8.66 mg/g, proving a great enhancement of adsorption ability with H_2O_2 treatment. Three adsorption models were applied to study the adsorption kinetics of MB on MCC, including pseudo first order model, pseudo second order model, and intraparticle diffusion model, which were adopted from Song, et al. [27]. Results summarized in Table 1 suggested that the adsorption of MB on MCC material was best described by pseudo second order model with a higher correlation of coefficient. In addition, calculated capacity (q cal) of 13.8 mg/g which was in agreement with the experimental value (Q exp) of 13.5 mg/g.
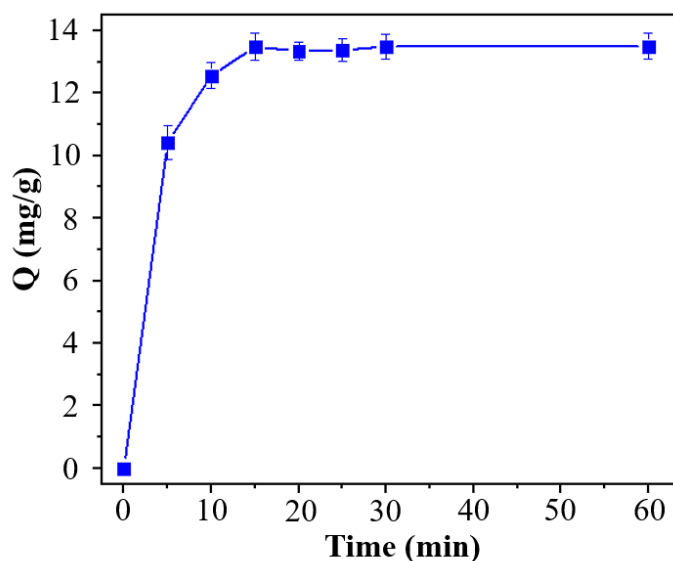

Figure 6 Effect of experiment time on MB adsorption (experimental condition: 30 mg MCC, 10 ppm MB, pH 7, and room temperature of ~ 30 ºC)

Table 1 Parameters for different adsorption kinetic models

Kinetic models	Linear form	R^2	(q ,cal) mg/g	K
Pseudo first order model	y = -0.1188x + 0.2719	0.7086	1.31	0.1188 (min^{-1})
Modified pseudo first order model	y = -0.1161 + 1.1643	0.7133	3.20	0.1161 (min^{-1})
Pseudo second order model	y = 0.0726x + 0.0625	0.9994	13.8	0.0843 ($g.mg^{-1}\ min^{-1}$)
Intraparticle diffusion model	y = 0.4452x + 10.85	0.4875	-	0.4452 ($mg.g^{-1}\ min^{-1}$)

pH is an important factor controlling the adsorption process. There is often a suitable pH range for high adsorption capacity since pH affects both the surface charge of adsorbent and the species of the adsorbate. The effect of solution pH on the adsorption process was investigated in a pH range of 3 – 10 and demonstrated in Figure 7a. The adsorption of MB was very low with a capacity of approximately 1 mg/g at a low pH range of 3 – 4, which could be due to the adsorption competition of H^+ and MB [46]. The adsorption capacity of the material increased rapidly in the range of pH 4 to pH 6, mostly because of the decrease of H^+ ion in the solution. As can be seen in Figure 7b, the point of zero charge of MCC was determined at 4.8. When pH > pH_{pzc} the surface of the MCC material was negatively charged, which could promote the interaction between the MCC surface and MB [46]. Therefore, pH 6 was chosen for further investigation.
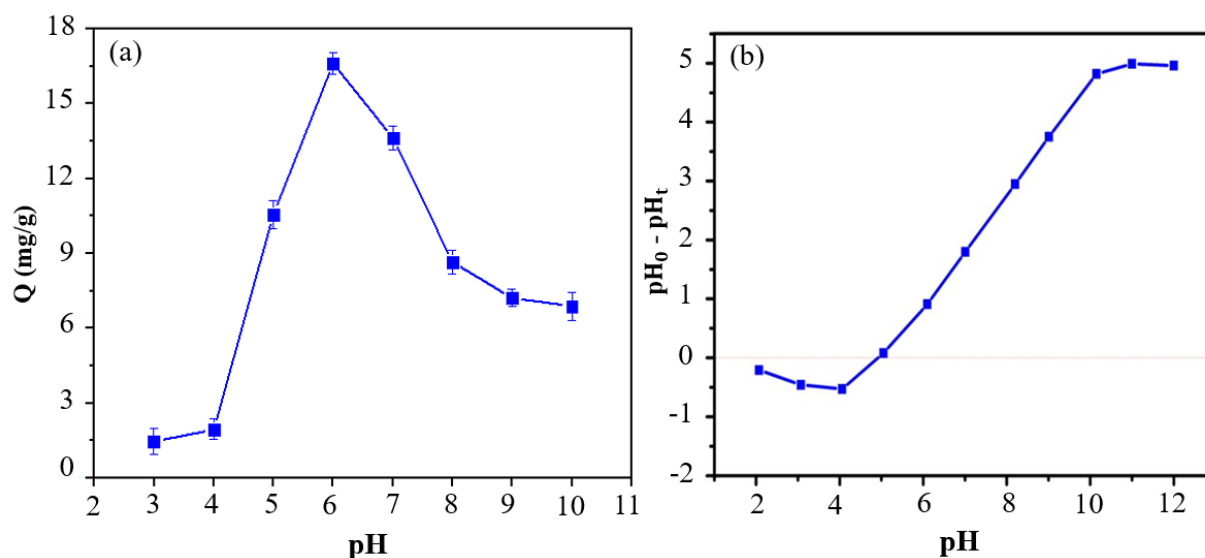

Figure 7 (a) Effect of solution pH on MB adsorption of MCC (experimental condition: 15 min, 30 mg MCC, 10 ppm MB, and room temperature of ~ 30 °C), and (b) the isoelectric point of MCC material

Choosing a suitable amount of absorbent is important, whose criteria are usually required both adsorption efficiency and acceptable adsorption capacity. The effect of MCC dosage on the removal of MB is depicted in Figure 8. It is usually that the removal efficiency increases from 51.9 to 100% but adsorption capacity decreases from 26.0 to 8.35 mg/g with increased dosage of MCC from 0.2 to 1.2 g/L because of more available adsorption site [47]. The excess adsorbent was observed with an MCC dosage of ≥ 0.6 g/L with adsorption efficiency of 100%. Therefore, the MCC dosage was chosen at 0.6 g/L for further experiments.
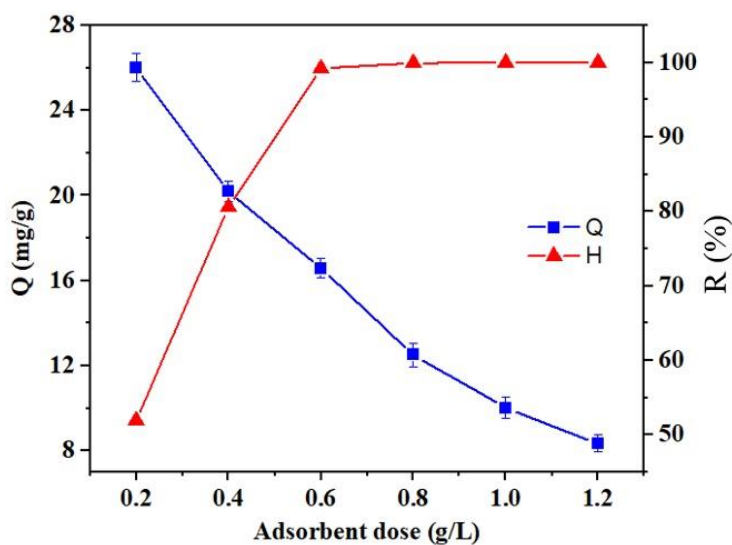

Figure 8 Effect of MCC dosage on the adsorption of MB (experimental condition: 15 min, 10 ppm MB, pH 6, and room temperature of ~ 30 °C)

It is widely known that the initial concentration of adsorbate has a strong effect on the adsorption capacity of the adsorbent due to phase equilibrium. The effect of MB concentration on the adsorption capacity of MCC material is exhibited in Figure 9. It was obvious that the adsorption capacity continuously increased from 8.31 to 40.9 mg/g when MB concentration increased from 5 to 40 mg/L. The experimental data were also fitted with Langmuir and Freundlich isotherms to find out the suitable adsorption model which followed the calculation step reported in the work of Phan, et al. [48]. Table 2 shows that the adsorption of MB on MCC material is more suitable with Langmuir isotherm because of its R^2 value of 0.9701 which was higher than that of Freundlich (0.9595). It could be concluded that the adsorption of MB on MCC is more likely to be monolayer adsorption. The maximum adsorption capacity was also compared with those reported previously and the results are presented in Table 3. This MCC material has a relatively high maximum adsorption capacity that other materials, except for Oil palm frond MCC powder and Salix babylonica leaves powder.
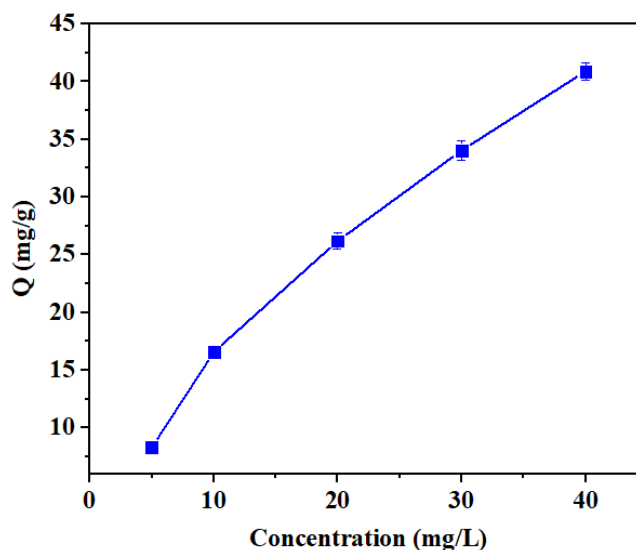

Figure 9 Effect of initial MB concentration on the adsorption ability of MCC (experimental condition: 15 min, 30 mg MCC, pH 6, and room temperature ~ 30 °C)

Table 2 Adsorption isotherm parameters

Isotherm	Parameter	Value
Langmuir	Q_{max} (mg/g)	40.161
	K_L (L/mg)	1.3387
	R^2	0.9701
	χ^2	0.0137
Freundlich	K_F ((mg/g)(L/mg)n)	27.042
	N	11.223
	R^2	0.9595
	χ^2	1.1852

Table 3 A comparison between Q_{max} in this study and previous researches

Adsorbent	Qmax MB (mg/g)	Reference
Commercial MCC	4.95	[49]
Immobilized oil palm frond MCC	11.42	[50]
Immobilized oil palm frond MCC (OPF-MCC)	12.85	[51]
Orange peel cellulose	18.60	[52]
MCC with H_2O_2 treatment	40.16	This study
Oil palm frond MCC powder	51.81	[53]
Salix babylonica leaves powder	60.97	[54]

The effect of temperature on the adsorption of MB is displayed in Figure 10. In the temperature range from 20 to 45 °C, the adsorption capacity of MCC material increased from 22.2 to 28.9 mg/g. The capacity increased rapidly to 28.1 mg/g in a temperature range of 20 - 35 °C and then increased slowly in a range of 35 - 45 °C. Based on thermodynamic parameters calculated from the literature [48, 55], the thermodynamic parameters in this study are summarized in Table 4. The positive value of ΔH denotes that the adsorption of MB onto the MCC surface is endothermic, which is more active under higher temperature [56]. Moreover, higher temperature creates more turbulence and diffusion but less viscous, which promotes the diffusion of MB inside the pore of the MCC material. The positive ΔS value shows the increased randomness at the solid-solution interface during the adsorption process. In addition, the decrease in free Gibbs energy with the increase of adsorption temperature shows the favorable adsorption under higher temperatures. ΔG values at all temperatures were in negative values, which confirmed the spontaneous and feasibility of the adsorption of MB on MCC. The adsorption reaction is a spontaneous process at high temperature, and not requires any energy from an external source to uptake MB molecules onto the MCC surface [57].
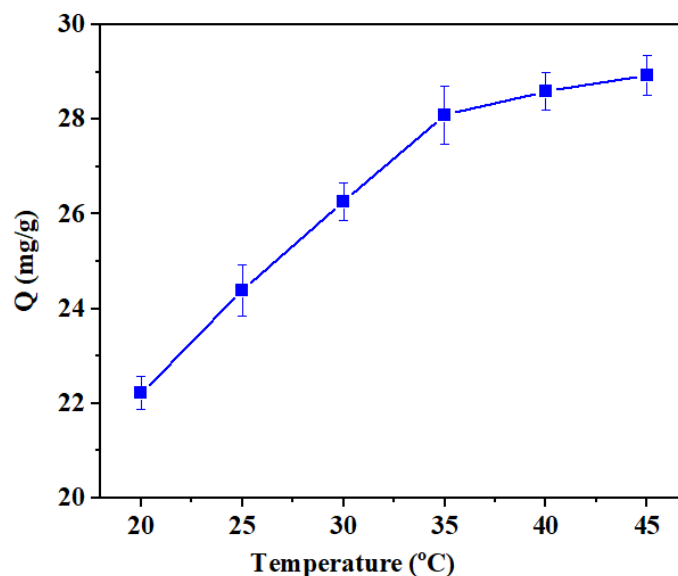
Figure 10 Effect of adsorption temperature on the adsorption of MB by MCC material (experimental condition: 15 min, 30 mg MCC, 20 ppm MB, pH 6)

Table 4 Thermodynamic parameters for adsorption of MB onto MCC

ΔH (kJ/mol)	ΔS (kJ/mol K)	ΔG (kJ/mol)					
		20	**25**	**30**	**35**	**40**	**45**
38.423	0.1316	-3.069	-3.777	-4.485	-5.193	-5.902	-6.610

The durability of the material is shown in Figure 11. It can be seen that MB removal efficiency tended to decrease with the number of the regeneration cycle. The MB removal efficiency decreased from 96% to 65% after 10 regeneration times. The tendency to reduce the efficiency of MB adsorption can be explained by the MB desorption process on the surface of MCC, which was incompletely due to MB still adhering to the material surface and obstructing the subsequent MB adsorption process [58].
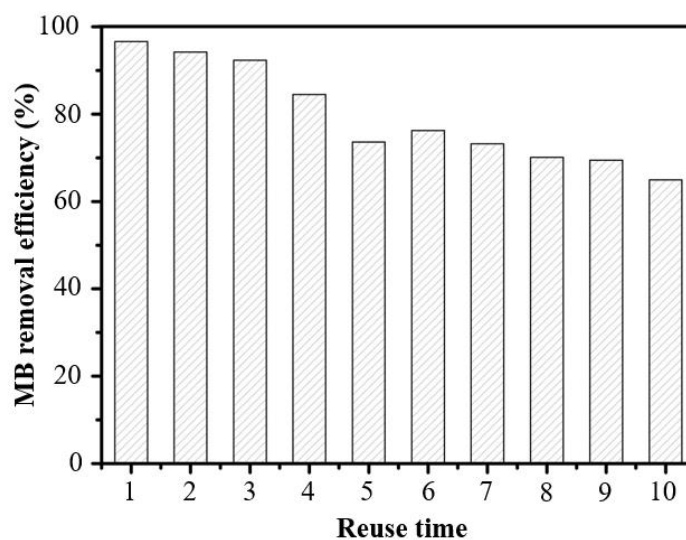

Figure 11 Reuse of MCC (experimental condition: 15 min, 30 mg MCC, 10 ppm MB, pH 6)

4. Conclusions

Microcrystalline cellulose with high quality was successfully synthesized by a green process and applied for the removal of MB in aqueous solution. Characteristics of synthetic materials are shown through SEM, FTIR, XRD, TGA, and BET analyses. The equilibrium time for MB adsorption was 15 min while the suitable solution pH was 6. The adsorption capacity increased with the increase of MB concentration and temperature but decreased with the increase of adsorbent dosage. The adsorption data fitted well with Langmuir isotherm and the maximum adsorption capacity (mg/g) of 40.16 mg/g was obtained at room temperature. These results suggested that MCC could be a very potential and green adsorbent for dye removal and wastewater treatment applications.

5. References

[1] Aurore G, Parfait B, Fahrasmane L. Bananas, raw materials for making processed food products. Trends Food Sci Tech. 2009;20(2):78-91.

[2] Vu HT, Scarlett CJ, Vuong QV. Phenolic compounds within banana peel and their potential uses: a review. J Funct Foods. 2018;40:238-48.

[3] Ahmad T, Danish M. Prospects of banana waste utilization in wastewater treatment: a review. J Environ Manag. 2018;206: 330-48.

[4] Pappu A, Patil V, Jain S, Mahindrakar A, Haque R, Thakur VK. Advances in industrial prospective of cellulosic macromolecules enriched banana biofibre resources: a review. Int J Biol Macromol. 2015;79:449-58.

[5] Danish M, Ahmad T, Majeed S, Ahmad M, Ziyang L, Pin Z, et al. Use of banana trunk waste as activated carbon in scavenging methylene blue dye: kinetic, thermodynamic, and isotherm studies. Bioresource Tech Rep. 2018;3:127-37.

[6] Thoorens G, Krier F, Leclercq B, Carlin B, Evrard B. Microcrystalline cellulose, a direct compression binder in a quality by design environment-a review. Int J Pharm. 2014;473:64-72.

[7] Iijima H, Takeo K. Handbook of hydrocolloids. In: Phillips GO, Williams PA, editors. Microcrystalline cellulose: an overview. Cambridge: Woodhead Publishing Ltd; 2000. p. 331-46.

[8] Trache D, Hussin MH, Hui Chuin CT, Sabar S, Fazita MRN, Taiwo OFA, et al. Microcrystalline cellulose: isolation, characterization and bio-composites application-a review. Int J Biol Macromol. 2016;93:789-804.

[9] Trusovs S, inventor. J H Biotech Inc., assignee. Microcrystalline cellulose. United States Patent US 6392034B1. 2002 May 21.

[10] Ibrahim MM, El-Zawawy WK, Juttke Y, Koschella A, Heinze T. Cellulose and microcrystalline cellulose from rice straw and banana plant waste: preparation and characterization. Cellulose. 2013;20(5):2403-16.

[11] Elanthikkal S, Gopalakrishnapanicker U, Varghese S, Guthrie JT. Cellulose microfibers produced from banana plant wastes: isolation and characterization. Carbohydr Polymer. 2010;80:852-9.

[12] Vijayalakshmi K, Devi BM, Latha S, Gomathi T, Sudha PN, Venkatesan J, et al. Batch adsorption and desorption studies on the removal of lead (II) from aqueous solution using nanochitosan/sodium alginate/microcrystalline cellulose beads. Int J Biol Macromol. 2017;104:1483-94.

[13] Vijayalakshmi K, Gomathi T, Latha S, Hajeeth T, Sudha PN. Removal of copper (II) from aqueous solution using nanochitosan/sodium alginate/microcrystalline cellulose beads. Int J Biol Macromol. 2016;82:440-52.

[14] Sango T, Cheumani Yona AM, Duchatel L, Marin A, Kor Ndikontar M, Joly N, et al. Step-wise multi-scale deconstruction of banana pseudo-stem (Musa acuminata) biomass and morpho-mechanical characterization of extracted long fibers for sustainable applications. Ind Crop Prod. 2018;122:657-68.

[15] Pereira ALS, Nascimento DMD, Souza Filho MDSM, Morais JPS, Vasconcelos NF, Feitosa JPA, et al. Improvement of polyvinyl alcohol properties by adding nanocrystalline cellulose isolated from banana pseudostems. Carbohydr Polymer. 2014;112:165-72.

[16] Bello K, Sarojini BK, Narayana B, Rao A, Byrappa K. A study on adsorption behavior of newly synthesized banana pseudo-stem derived superabsorbent hydrogels for cationic and anionic dye removal from effluents. Carbohydr Polymer. 2018;181:605-15.

[17] Shanmugam N, Nagarkar R, Kurhade M. Microcrystalline cellulose powder from banana pseudostem fibres using bio-chemical route. Indian J Nat Prod Resour. 2015;6(1):42-50.

[18] Pelissari FM, Amaral Sobral PJ, Menegalli FC. Isolation and characterization of cellulose nanofibers from banana peels. Cellulose. 2014;21:417-32.

[19] Cherian BM, Pothan LA, Nguyen-Chung T, Mennig G, Kottaisamy M, Thomas S. A novel method for the synthesis of cellulose nanofibril whiskers from banana fibers and characterization. J Agr Food Chem. 2008;56:5617-27.

[20] Li C, Liu G, Nges IA, Deng L, Nistor M, Liu J. Fresh banana pseudo-stems as a tropical lignocellulosic feedstock for methane production. Energ Sustain Soc. 2016;6:27.

[21] Jayaprabha JS, Brahmakumar M, Manilal VB. Banana pseudo stem characterization and its fiber property evaluation on physical and bio extraction. J Nat Fiber. 2011;8:149-60.

[22] Garba ZN, Lawan I, Zhou W, Zhang M, Wang L, Yuan Z. Microcrystalline cellulose (MCC) based materials as emerging adsorbents for the removal of dyes and heavy metals-a review. Sci Total Environ. 2020;717:135070.

[23] Phan PT, Nguyen TT, Nguyen NH, Padungthon S. Triamine-bearing activated rice husk ash as an advanced functional material for nitrate removal from aqueous solution. Water Sci Tech. 2019;79:850-6.

[24] Rasheed M, Jawaid M, Karim Z, Abdullah LC. Morphological, physiochemical and thermal properties of microcrystalline cellulose (mcc) extracted from bamboo fiber. Molecules. 2020;25:2824.

[25] Mahmood T, Saddique MT, Naeem A, Westerhoff P, Mustafa S, Alum A. Comparison of different methods for the point of zero charge determination of NiO. Ind Eng Chem Res. 2011;50:10017-23.

[26] Kosmulski M. pH-dependent surface charging and points of zero charge II. Update. J Colloid Interface Sci. 2004;275:214-24.

[27] Song W, Gao B, Xu X, Wang F, Xue N, Sun S, et al. Adsorption of nitrate from aqueous solution by magnetic amine-crosslinked biopolymer based corn stalk and its chemical regeneration property. J Hazard Mater. 2016;304:280-90.

[28] Ayawei N, Ebelegi AN, Wankasi D. Modelling and interpretation of adsorption isotherms. J Chem. 2017;2017:3039817.

[29] Shahbazi A, Younesi H, Badiei A. Functionalized SBA-15 mesoporous silica by melamine-based dendrimer amines for adsorptive characteristics of Pb (II), Cu (II) and Cd (II) heavy metal ions in batch and fixed bed column. Chem Eng J. 2011;168:505-18.

[30] Paul SA, Piasta D, Spange S, Pothan LA, Thomas S, Bellmann C. Solvatochromic and electrokinetic studies of banana fibrils prepared from steam-exploded banana fiber. Biomacromolecules. 2008;9:1802-10.

[31] Fatrozi S, Purwanti L, Sari SK, Ariesta MN, Marliyana SD. Properties of starch bio foam reinforced with microcrystalline cellulose from banana stem fiber. AIP Conf Proc. 2020;2237(1):020054.

[32] Camacho W, Karlsson S. NIR, DSC, and FTIR as quantitative methods for compositional analysis of blends of polymers obtained from recycled mixed plastic waste. Polymer Eng Sci. 2001;41:1626-35.

[33] Aswin Kumar I, Viswanathan N. Development and reuse of amine-grafted chitosan hybrid beads in the retention of nitrate and phosphate. J Chem Eng Data. 2018;63:147-58.

[34] Silva SS, Duarte ARC, Carvalho AP, Mano JF, Reis RL. Green processing of porous chitin structures for biomedical applications combining ionic liquids and supercritical fluid technology. Acta Biomaterialia. 2011;7:1166-72.

[35] Wanrosli W, Rohaizu R, Ghazali A. Synthesis and characterization of cellulose phosphate from oil palm empty fruit bunches microcrystalline cellulose. Carbohydr Polymer. 2011;84:262-7.

[36] Choi M, Kang YR, Lim IS, Chang YH. Structural characterization of cellulose obtained from extraction wastes of Graviola (Annona Muricata) leaf. Prev Nutr Food Sci. 2018;23:166-70.

[37] Oh SY, Yoo DI, Shin Y, Seo G. FTIR analysis of cellulose treated with sodium hydroxide and carbon dioxide. Carbohydr Res. 2005;340:417-28.

[38] Xiong R, Zhang X, Tian D, Zhou Z, Lu C. Comparing microcrystalline with spherical nanocrystal line cellulose from waste cotton fabrics. Cellulose. 2012;19:1189-98.

[39] Murigi M, Madivoli E, Mathenyu M, Kareru P, Gachanja A, Njenga P, et al. Comparison of physicochemical characteristics of microcrystalline cellulose from four abundant Kenyan biomasses. IOSR J Polymer Textill Eng. 2014;1:53-63.

[40] Correa AC, de Morais Teixeira E, Pessan LA, Mattoso LHC. Cellulose nanofibers from curaua fibers. Cellulose. 2010;17: 1183-92.

[41] Fisher T, Hajaligol M, Waymack B, Kellogg D. Pyrolysis behavior and kinetics of biomass derived materials. J Anal Appl Pyrol. 2002;62:331-49.

[42] Rosa SML, Rehman N, de Miranda MIG, Nachtigall SMB, Bica CID. Chlorine-free extraction of cellulose from rice husk and whisker isolation. Carbohydr Polymer. 2012;87(2):1131-8.

[43] Wang Y, Zhao Y, Deng Y. Effect of enzymatic treatment on cotton fiber dissolution in NaOH/urea solution at cold temperature. Carbohydr Polymer. 2008;72:178-84.

[44] Abe K, Yano H. Comparison of the characteristics of cellulose Micro fibril aggregates of wood, rice straw and potato tuber. Cellulose. 2009;16:1017-23.

[45] Park S, Baker JO, Himmel ME, Parilla PA, Johnson DK. Cellulose crystallinity index: measurement techniques and their impact on interpreting cellulase performance. Biotechnol Biofuels. 2010;3:10.

[46] Somsesta N, Sricharoenchaikul V, Aht-Ong D. Adsorption removal of methylene blue onto activated carbon/cellulose biocomposite films: equilibrium and kinetic studies. Mater Chem Phys. 2020;240:122221.

[47] Abd Rashid R, Jawad AH, Azlan M, Ishak M, Kasim NN. FeCl$_3$-activated carbon developed from coconut leaves: characterization and application for methylene blue removal. Sains Malaysiana. 2018;47(3):603-10.

[48] Phan PT, Nguyen TT, Nguyen NH, Padungthon S. A simple method for synthesis of triamine-sio2 material toward aqueous nitrate adsorption. Environ Nat Resour Res. 2019;17(4)59-67.

[49] Tan KB, Abdullah AZ, Horri BA, Salamatinia B. Adsorption mechanism of microcrystalline cellulose as green adsorbent for the removal of cationic methylene blue dye. J Chem Soc Pakistan. 2016;38(4):651-64.

[50] Tan CHC, Sabar S, Haafiz MM, Garba ZN, Hussin MH. The improved adsorbent properties of microcrystalline cellulose from oil palm fronds through immobilization technique. Surface Interfac. 2020;20:100614.

[51] Tan CHC, Sabar S, Hussin MH. Development of immobilized microcrystalline cellulose as an effective adsorbent for methylene blue dye removal. S Afr J Chem Eng. 2018;26:11-24.

[52] Annadurai G, Juang RS, Lee DJ. Use of cellulose-based wastes for adsorption of dyes from aqueous solutions. J Hazard Mater. 2002;92:263-74.

[53] Hussin MH, Pohan NA, Garba ZN, Kassim MJ, Rahim AA, Brosse N, et al. Physicochemical of microcrystalline cellulose from oil palm fronds as potential methylene blue adsorbents. Int J Biol Macromol. 2016;92:11-9.

[54] Khodabandehloo A, Rahbar-Kelishami A, Shayesteh H. Methylene blue removal using *Salix babylonica* (Weeping willow) leaves powder as a low-cost bio sorbent in batch mode: kinetic, equilibrium, and thermodynamic studies. J Mol Liq. 2017;244:540-8.

[55] Duranoglu D, Trochimczuk AW, Beker U. Kinetics and thermodynamics of hexavalent chromium adsorption onto activated carbon derived from acrylonitrile-divinylbenzene copolymer. Chem Eng J. 2012;187:193-202.

[56] Singh KP, Gupta S, Singh AK, Sinha S. Optimizing adsorption of crystal violet dye from water by magnetic nanocomposite using response surface modeling approach. J Hazard Mater. 2011;186:1462-73.

[57] Rashid RA, Jawad AH, Ishak MAM, Kasim NN. KOH-activated carbon developed from biomass waste: adsorption equilibrium, kinetic and thermodynamic studies for Methylene blue uptake. Desalination Water Treat. 2016;57:27226-36.

[58] Du X, Han Q, Li J, Li H. The behavior of phosphate adsorption and its reactions on the surfaces of Fe-Mn oxide adsorbent. J Taiwan Inst Chem Eng. 2017;76:167-75.